

## **Quantitative Model of Cellulite: Three Dimensional Skin Surface Topography, Biophysical Characterization and Relationship to Human Perception**

Lola K. Smalls, BS<sup>1,2</sup>, Caroline Y. Lee<sup>1</sup>, Jennifer Whitestone, MS<sup>3</sup>, W. John Kitzmiller, MD<sup>1,4</sup>, R. Randall Wickett, PhD<sup>1,2</sup>, Marty O. Visscher, PhD<sup>1</sup>  
The Skin Sciences Institute, Cincinnati Children's Hospital Research Foundation,<sup>1</sup>  
College of Pharmacy<sup>2</sup>, College of Medicine<sup>4</sup>, University of Cincinnati, Cincinnati, OH,  
<sup>3</sup>Total Contact, Germantown, OH

### **Abstract**

Gynoid lipodystrophy (cellulite) is the uneven distribution of subcutaneous tissue giving rise to an irregular, dimpled skin surface of the thighs, abdomen, and buttocks in 85% of post-adolescent women. We hypothesized that the distinctive surface morphology results when subcutaneous adipose tissue protrudes into the lower reticular dermis, thereby creating irregularities at the surface. Epidermal and dermal tissue biomechanical properties may also influence cellulite severity. Cellulite-affected sites were evaluated using a combination of noninvasive biophysical measurements in populations of 51 females with varying degrees of cellulite, 11 non-cellulite controls, and 10 male controls and the specific factors that contributed to cellulite severity were determined. We used a novel non-contact laser surface scanner to capture high resolution three-dimensional scans and quantify the skin surface morphology and determine specific roughness values. The surface images were assessed by experts and naïve judges (n = 62). Also measured were body composition via dual-energy x-ray absorptiometry, dermal thickness and dermal-subcutaneous junction via high resolution 3D ultrasound, surface photography under compression, and biomechanical properties. The roughness parameters Svm (mean depth of the lowest valleys) and Sdr (ratio between the roughness surface area and the area of the xy plane) were highly correlated to the expert image grades and were designated as the quantitative measures of cellulite severity. The naïve judge and expert grades were also highly correlated. The strength of the correlations among naïve grades, expert grades, and roughness measures confirmed that the data quantitatively assesses human perception of cellulite and can, therefore, be used to guide development and evaluation of treatment modalities. Cellulite severity was correlated to BMI, thigh circumference, percent thigh fat, and the architecture of the dermal-subcutaneous border (ultrasound surface area, red band SD from compressed images). Greater severity was positively related to compliance and negatively related to stiffness. Cellulite severity was *predicted* by the percent of fat in the subregion and the area of the dermal-subcutaneous border, but the biomechanical properties did not significantly contribute to prediction of severity. Comparison of parameters for females and males further suggest that percent thigh fat and surface area roughness deviation are the distinguishing features of cellulite, given the control for BMI and age in the comparisons.

## **Introduction**

Gynoid lipodystrophy (cellulite), the unattractive cottage cheese-like dimpling of the skin of the thighs, abdomen, and buttocks, affects 85% of post-adolescent women(1, 2). Cellulite treatment is a high priority for the pharmaceutical and cosmetic industries (2-9) (10). Products (11-15), supplements (16), and massage techniques (8, 9) purport to treat the condition, presumably by reducing the appearance of the dimpled, lumpy skin. The lumpy skin surface texture is attributed to the three dimensional (3D) architecture of the hypodermal connective tissue (14, 17-20). In females, fat cell chambers, “papillae adiposae”, are sequestered by connective tissue septa, positioned in a radial and arched manner, and anchoring the dermis to the muscle fascia. The subcutaneous fat cell chambers bulge into the dermis, thereby changing the appearance of the skin surface (ref 13). Cellulite is not specific to overweight females but added weight may cause enlargement of the fat lobules, further protrusion into the dermis and exacerbation of the condition (2, 17). Weight loss is reported to diminish cellulite, but it may not alter the underlying dermal-subcutaneous structures (17, 19). The literature on the etiology of cellulite and on the effectiveness of treatments to ameliorate the condition is limited (4, 6, 14, 16, 21), given the prevalence of the problem. The relationships among histological and biophysical skin characteristics of cellulite have not previously been reported. Identification of key factors responsible for the visual appearance of cellulite will help to facilitate development and selection of effective treatments.

We hypothesized that skin surface characteristics of cellulite result when subcutaneous adipose tissue protrudes into the lower reticular dermis, thereby creating irregularities at the epidermal surface. The biomechanical properties of the epidermis and dermis may also influence the severity. We conducted a set of noninvasive biophysical measurements of the cellulite-affected tissue and determined the specific factors that contribute to cellulite severity. The surface morphology was quantified using a novel, non-contact three-dimensional laser scanning system to generate surface roughness parameters and provide a standardized measure of severity. In the literature, cellulite severity is generally evaluated with various visual and photographic methods, although accepted standards have not yet emerged. We related the technical measures of severity to naïve and subject assessment using typical 0-9 category scales. Quantitative, reproducible methods will facilitate effective comparison of treatments across studies. Furthermore, treatment effectiveness will be judged by the patient/consumer based on the impact on cellulite severity and appearance. Ultimately, evaluation methods must be linked to human perception of severity and change.

## **Materials and Methods**

### *Subjects*

Fifty-one (51) females with visible cellulite were recruited from several weight loss programs (medication, liquid diet, low-fat meals, Weight Watchers and bariatric surgery). Eleven (11) females without visible cellulite were controls. Individuals who were pregnant, had an active skin condition (e.g., rash, wound) on the thigh, or had been treated for cellulite within three months were excluded from participation. The Institutional Review Boards of Cincinnati Children’s Hospital Medical Center and the

University of Cincinnati approved the study protocol. All subjects provided written informed consent for study participation.

Ten (10) males, matched to the female subjects for BMI and age, were recruited as additional controls to evaluate the effect of gender on the three-dimensional and biophysical characteristics of the thigh. All subjects signed written informed consent. The thigh regions of interest were shaved with electric clippers prior to measurements.

Sixty-two (62) females with no knowledge of the cellulite research were recruited as naïve judges from the general population. They evaluated the thigh images collected from the study population for severity using a 0-9 category scale. The study subjects provided written consent for evaluation of their cellulite images by the judges.

#### *Three Dimensional Skin Surface Topography*

Three dimensional (3D) skin surface data were obtained with a Cyberware Rapid 3D Digitizer (Cyberware, Inc., Monterrey, CA) mounted on a linear platform and controlled by CyScan data acquisition software. The scanner operates on the principal of triangulation. As a helium-neon laser light source passes through two cylindrical lenses, the resulting vertical plane of light projects onto the surface of the object being scanned. The highlighted profile is reflected from the image mirrors to a video sensor and digitized in a raster fashion to determine the two-dimensional (2-D) coordinates of 256 points along the profile surface. The scanner moves along a linear trajectory performing 512 individual surface contour scans in equal increments. Trigonometric calculations of the 2-D coordinates to three-dimensional (3-D) space are performed.

The outer aspects of both thighs were scanned while subjects sat on a level surface with knees bent at a 90° angle (402 X 170 mm in < 40 sec. at 0.5 x 0.38 mm planar resolution). With the aid of a special motor controlled platform, the scanner platform was raised and lowered to allow accurate positioning of the subject within the scan area. The quantitative surface roughness parameters were obtained from the scan data using a customized version of TrueMap Software (TrueGage, N. Huntingdon, PA). The images were first processed to remove non-cellulite features. The form removal utility applied a LS 3<sup>rd</sup> order polynomial equation to remove the thigh curvature. The filtering utility set at 0.25 mm removed noise due to movement, hair, and varicose veins. Remaining anomalies are removed with an outlier routine. The surface roughness parameters (Table 1) are calculated for the region of interest (10.7 x 11.3 cm, center of the thigh) (22).

#### *Visual Scoring of Cellulite*

Expert Image Scores: Three research team members reviewed two sets of 66 3D shaded (grey scale) scans that covered the range of severities observed in the general population. They identified the cellulite features and developed a ten-point classification scale of cellulite severity (0-9) wherein [0] represented no cellulite, [1,2,3] indicated varying degrees of slight cellulite, [4,5,6] were moderate, and [7,8,9] were severe. From the database, we selected ten images, representing each point (0-9), for evaluation by naïve judges and established the ten images as the Expert Image Grading Scale.

Live Visual Grades: The lateral thighs were evaluated with the subject positioned on a bicycle seat (to avoid thigh compression) with the knee at 90° angles. A trained judge graded the outer aspect of each thigh using a five-point scale (0-4), with half point increments for intermediate conditions. The scale was 0 (smooth, no dimples), 1 (shallow, small visible dimples, few and sparsely located), 2 (moderate number visible dimples, some may be large), 3 (large number dimples, many large, over most of the surface, cottage cheese appearance), and 4 (wide, deep visible dimples over entire thigh, very prominent cottage cheese appearance).

#### *Measurements*

The weight, height, and thigh circumference were measured using a standard hospital scale with height bar and measuring tape. Sites at the center lateral thighs were demarcated with a 2 cm diameter region centered within a 5 cm diameter circle.

#### *Dual Energy X-Ray Absorptiometry (DEXA)*

Total and regional body composition (lean and fat mass) was measured with a dual energy x-ray absorptiometry (DEXA) total body scanner (Hologic Inc., San Francisco, CA) at the body core composition laboratory of the General Clinical Research Center of Cincinnati Children's Hospital Medical Center. Fat percentages were calculated for the total body, thigh, thigh subregion (area of ultrasound and biomechanical measurements), android (torso) and gynoid (hip/thigh). The regional sites were analyzed using joints as landmarks. The body fat distribution was calculated from the android/gynoid fat mass ratio, an index of the fat allocation amid the torso and hip/thigh regions (23).

#### *Ultrasound*

Dermal thickness (mm) and dermal-subcutaneous junction surface area of the thigh sites were quantified using the Dermascan C<sup>®</sup> Version 3 (Cortex Technology, Hadsund, Denmark) with a 20 MHz 3D probe (24). A 22.4 x 22.4 mm area was scanned with an interslice distance of 0.2 mm, providing 112 B-scans (2D images). The acoustic velocity of the instrument was set to 1580 m/s (24). The mean dermal thickness (112 B-Scans) was determined with the Dermascan C<sup>®</sup> software system to define the outer boundary of the epidermis and the inner dermal/subcutaneous fat boundary. The surface area of the 3D dermal/subcutaneous junction was reconstructed by manually delineating the dermal/subcutaneous border from 50 consecutive B-Scans (224mm<sup>2</sup> area or 50 scans x 0.2mm *z-dir* x 22.4 mm *y-dir*).

### *Surface Texture with Photography*

Surface texture under compression were measured with the Accentuated Cellulite Imaging System (ACIS, Procter and Gamble, Cincinnati, OH) The thigh skin was compressed with gripping handles to 11.6mm from a starting point of zero. Moisturizing lotion (Oil of Olay Beauty Fluid, Procter and Gamble, Cincinnati, Ohio) was applied prior to the measurement to eliminate confounding effects of dry skin. The digital images were color corrected and processed (Optimas software). A center region (570 x 210 mm) was analyzed to eliminate edge effects. Changes in color intensity of adjacent pixels provided an output parameter Red Band Standard Deviation (Red Band SD), related to shadowing in cellulite dimples under compression. .

### *Biomechanical Properties*

The biomechanical properties were measured on the midlateral thighs (2 cm diameter circle) using the BTC-2000™ (SRLI Technologies, Nashville, TN) through two cycles over 2 cm at a pressure of 10mmHg/second for 15 seconds (150mmHg, 200mbar) with 5 seconds of relaxation between cycles. The properties were laxity (acute elastic deformation), laxity % (percent, indicates slack or looseness), elastic deformation (total displacement at maximum pressure), stiffness (slope of the stress/strain curve, higher value indicates tighter skin), energy absorption (area under the stress/strain curve, entire deformation response, high values indicate more compliant skin), elasticity (reverse deformation by the full pressure release), and elasticity % (elasticity/elastic deformation x 100%, high values indicate more elastic skin) (25).

### *Naive Judge Cellulite Image Assessment*

High contrast (grey scale) images were viewed on black backgrounds to allow the judge to focus on the image and distinguish the skin surface features. Length of time was optimized to minimize fatigue and maximize response fidelity. Answer sheets were designed to facilitate ease of use. Judges were given descriptors of cellulite (lumps, bumps, dimples, ripples, cottage cheese appearance) at the start of the session and instructed to ignore non-cellulite features (e.g., vertical bands, specks). Responses were recorded using a ten-point, 0-9 category scale (Table 2).

Four different assessments (Tests A-D) were used to randomize presentation and ensure that question sequence did not affect image scoring of cellulite severity. Judges first viewed single images to provide them with a frame of reference. They evaluated the ten single images of the Expert Image Grading Scale on the scale. Use of pair-wise comparisons is more effective than subjective rating scales in medical imaging by allowing observers to detect small differences in image quality (26). Therefore, we used a modified version of the two-alternative forced-choice (TAFC) method where judges were required to score each image within a pair. The method assumes that the image with the higher score had the more severe condition (26). Twenty-five (25) randomized pairs of varying severity differences were evaluated to assess the threshold of detection of incremental differences (i.e. grade 1 vs. 7, 6-increment difference). Identical image pairs were included as a control.

### *Statistical Analysis*

The data were analyzed using the Sigma Stat Software (SPSS, Inc.) with a significance level of  $p \leq 0.05$ . Results are represented as mean  $\pm$  SD and mean  $\pm$  SEM. Student's t-test was used for comparison of two different groups. Correlation coefficients were computed using Pearson Product Moment or Spearman procedures (non-normally distributed data) to evaluate relationships among parameters. Multiple linear regression analyses were performed to determine the ability of a combination of independent variables to predict the dependent variable.

## **Results**

### *Quantitation of Cellulite Severity*

Selection criteria for the ten final images of the Expert Image Grading Scale (Figure 1) included: depth of dimples, area of coverage, and cottage-cheese-like appearance. Correlation of the expert image grades with the surface roughness parameters (Table 3) indicated the highest association (correlation coefficient = 0.86,  $p = 0.001$ ) for parameter Svm (Figure 2). Parameter Sdr was also highly correlated with expert image score (correlation coefficient = 0.86). Multiple linear regression analyses showed that inclusion of the non-correlated variables Ssk and Sku did not add significantly to either model. Weight, age, or the interaction term (weight\*age) did not affect either Svm or Sdr. For Svm, the equation was:  $Image\ Score = -1.66 + (2.4 * Svm)$ , with values of R,  $R^2$ , and adjusted  $R^2$  of 0.86, 0.75, and 0.71, respectively. For Sdr, the equation was  $Image\ Score = 1.25 + (388 * Sdr)$ , with values of R,  $R^2$ , and adjusted  $R^2$  of 0.86, 0.73, and 0.70, respectively. The live expert visual grades (0-4) for the ten thighs in the Expert Image Scale were highly correlated to the expert image scores ( $r = 0.92$ , Table 3). The highest correlation was for Sdr ( $r = 0.89$ ), indicating that this parameter is sensitive to human visual perception.

The naïve judges scored the images lower than experts, presumably because they were processing the data in a bottom-up fashion, i.e., perception are formed based on the data in the images. The naïve judge mean scores and the expert grades for the ten images were highly correlated ( $r = 0.96$ ) and not significantly different. Svm and Sdr had the highest correlations to expert and naïve scores ( $r \geq 0.86$ ) (Figure 3). The naïve judges and experts agreed on the paired image assessments, although the experts noted larger differences. This result is not surprising, given the experts' experience in reviewing 3D laser scans of cellulite. The experts used top-down processing, i.e., perceptions are formed based upon expectations and from previous knowledge with the range of severity.

### *Biophysical Characterization of Cellulite*

Fifty-six (56) females completed the measurements. The mean BMI (kg/m<sup>2</sup>) was  $34.6 \pm 8$  (range 21 - 57) and the mean weight was  $204 \pm 52$  (range 128 - 331). The mean age was  $44.3 \pm 8$  (range 21- 60). For the males, the mean BMI was  $33.2 \pm 6$  kg/m<sup>2</sup> and the mean age was  $41.8 \pm 11.2$  years.

Table 4 shows the results (mean  $\pm$  standard error, range) of the biophysical evaluations for females and males. Good correlations were found between expert image grades and

quantitative roughness. Svm, Sz, and Spm had the highest correlations with image score (females), and correlation coefficients were 0.69 ( $p < 0.001$ ), 0.68 ( $p < 0.001$ ), and 0.62 ( $p < 0.001$ ), respectively.

The biophysical factors that related to cellulite severity were identified from the correlation coefficients among all of the measurements (Table 5, coefficients of  $\cong 0.4$  or higher,  $p < 0.05$ ). Cellulite severity, as measured by either surface roughness (Svm) or by live visual grade, was correlated to BMI (weight), thigh circumference, percent thigh fat, and the architecture of the dermal-subcutaneous border (ultrasound surface area, red band SD from compressed images). Greater cellulite severity was positively associated with greater tissue compliance and negatively associated with stiffness (less stiff, greater severity).

The parameters that impact or predict cellulite severity were identified from multiple linear regression modeling procedures. Expert Image Score and Svm were chosen as the quantitative measures of cellulite severity (dependent variable) and models with the highest R and  $R^2$  values are reported. The Expert Image Score could be predicted from subregion % fat ( $p < 0.001$ ) and Sdr ( $p = 0.01$ ), giving the equation:  $Image\ Score = -4.2 + (0.22 * Subregion\ \% Fat) + (0.91 * Sdr)$ . The values of R,  $R^2$ , and adjusted  $R^2$  were 0.82, 0.68 and 0.67, respectively. Cellulite severity (Svm) could be predicted from subregion %fat ( $p < 0.001$ ) and dermal-subcutaneous surface area ( $p = 0.02$ ). The equation was:  $Svm = -2.2 + (0.08 * Subregion\ \% Fat) + (0.006 * D-S\ surface\ area)$ , with R,  $R^2$ , and adjusted  $R^2$  values of 0.68, 0.46 and 0.44, respectively.

#### *Male and Female Comparisons*

Ten females, matched for BMI and age, were selected at random for comparison to the males. A second group of BMI and age matched females was used to further verify the are results. The average BMI ( $kg/m^2$ ) for the males was  $33.2 \pm 6$ , compared to  $33.4 \pm 6$  and  $33.0 \pm 5.9$  for the two female groups. T-test analyses confirmed that the groups were comparable for BMI and age.

The males and females (both groups) differed significantly in body composition ( $p < 0.001$ ) (Table 4). The mean subregion % fat was  $20.3 \pm 5.4\%$  for males and  $36.5 \pm 7.2\%$  and  $33.8 \pm 9.3\%$  for the females. The mean thigh % fat was  $29.0 \pm 6.1\%$  for males and  $44.5 \pm 5.8\%$  and  $42.0 \pm 7.3\%$  for females. One female group had a directionally higher ( $p = 0.10$ ) live visual cellulite grade than the males. No significant differences were found for expert image score, thigh circumference, dermal thickness, dermal-subcutaneous surface areas, or any of the biomechanical properties. With respect to cellulite severity, the males and females differed significantly in Sdr ( $p < 0.005$ ), with Sdr substantially greater for females than for males (Figure 4).

#### **Discussion**

Three dimensional skin surface microstructures, e.g., wrinkles, have been quantified by a variety of techniques (27-30). Many use replicas of the skin surface coupled with mechanical, laser, optical or interference fringe profilometry to evaluate roughness

parameters. For cellulite, the area of interest is substantially larger and the limitations of the replica methods become significant. Akazaki et al described an optical system that could make direct skin measurements over a 6.4 mm<sup>2</sup> area with a high resolution of 12.5 μm (28). Optical profilometry with CDD sensors allows measurement of depths up to 6 mm (27) and interference fringe projection methods have a 1 mm depth of field (29). These distances are smaller than those encountered with cellulite. Three dimensional skin surface features have been reported using the non-contact PRIMOS system, which projects parallel stripes onto the surface and determines the third dimension from differences in elevation between the projections and the skin (31, 32). Quantitative roughness parameters in the μm range and within a sampling area of 2.4 x 3.0 cm can be measured by this method, indicating the suitability for micro textures.

The three dimensional features of the face and head have been measured with non-contact laser surface scanning systems that record the x,y,z coordinates of multiple points across the surface (33, 34). Changes in the range of 2-3 mm could be accurately measured over a relatively large surface area. Rohmer et al recently used fringe projection methods to quantify roughness parameters and volume of cellulite affected skin (35). A system to directly measure 3D surface features and quantified wrinkle depth and width has been reported (28). The maximum distance from top to bottom with the skin area was defined as wrinkle depth and this parameter was similar to St (vertical distance from the highest peak to the deepest valley) in this report. We used a novel, non-contact three-dimensional laser surface scanner (resolution of 0.5 mm) to generate surface roughness parameters and to provide a standardized, reproducible measure of severity. This system has been used to quantify the surface features of wounds and burn scars and to generate 3D data for the construction of burn masks (36). Since the laser scanning technique does not use shadows to create the 3D image, difficulties with lighting were avoided. The 3D surface images could easily be rotated with the software to provide the investigator with multiple views of the cellulite. The subject position on a rigid platform provided natural thigh compression.

The roughness parameters Svm and Sdr were highly correlated with the expert image scores for a set of ten standard images. Therefore, they were designated as the quantitative measures of cellulite severity. *The strength of the agreements (a) between expert image scores and roughness values and (b) between live visual scores and the roughness parameters strongly indicates that the 3D laser scan and analysis methodology quantitatively characterizes cellulite.* The naïve judge and expert grades were highly correlated (r= 0.96) for the ten images and roughness parameters Svm and Sdr had the highest correlations to expert and naïve scores (r ≥ 0.86) (Figure 3). *The strength of the correlations among naïve grades, expert grades, and roughness measures confirms that the data quantitatively assesses human perception of cellulite and can, therefore, be used to guide development and evaluation of treatment modalities.* To our knowledge, this is the first report of a quantitative assessment of cellulite using a novel 3D laser scanning technology and to establish the relationship between quantitative measurements of cellulite severity and subject perception of the condition.

A combination of biophysical techniques, including standardized, expert clinical grading of photographs (wrinkling, rhytids, laxity/tone, etc), surface roughness parameters (Ra, Rz) from replicas, and subject assessment of improvement, have been used successfully to evaluate treatments on photo-damaged facial skin (37). Rao et al used a combination of high-quality digital photography (multiple angles, tangential lighting), expert image assessment (4 trained dermatologists), and subject self-assessment in a paired-comparison design to evaluate cellulite treatments (15). Surface features were captured from shadows at various angles but quantitative roughness values were not reported. Bertin et al concluded that a combination of techniques, including surface macro texture, biomechanical properties, cutaneous flowmetry, and dermal/hypodermal structure determination, were effective in measuring the effect of treatments on cellulite (6).

We found that cellulite severity, measured by expert image evaluation or quantitative surface roughness parameters, was significantly related to the body fat in the affected region, the architecture (surface area) of the dermal-subcutaneous border, and the tissue mechanical properties (compliance, stiffness). Body mass index and correlated anthropomorphic parameters (weight, thigh circumference) are highly associated with cellulite severity. The observed appearance of cellulite, i.e., cellulite severity as measured by surface roughness parameters, depends upon the percentage of fat in the region of interest (thigh) and the surface area of the dermal-subcutaneous junction. Cellulite severity was *predicted* by the percent of fat in the subregion and the area of the dermal-subcutaneous border. While the biomechanical properties of energy absorption and stiffness correlated with surface roughness, they did not significantly contribute to the severity. The contributions of subcutaneous fat to the condition of cellulite were reported by Mole et al (38). High frequency ultrasound coupled with a patient questionnaire indicated that cellulite is caused by defects in adipocyte biology and with the superficial fat tissues. Furthermore, the comparison of parameters for females and BMI and age-matched males provided key information regarding the factors that influence cellulite. The findings suggest that percent thigh fat and surface area roughness deviation are the distinguishing features of cellulite, given the control for BMI and age in the comparisons.

### **Acknowledgments**

This work was supported by grants from The Procter & Gamble Company and by USPHS GCRC Grant #M01 RR 08084 from the National Center for Research Resources, NIH. The authors wish to acknowledge Donna Buckley and Heidi Kalkwarf of the Cincinnati Children's Hospital GCRC, Jareen Meinzen-Derr of Cincinnati Children's Hospital for statistical guidance, Christopher Laffley of Total Contact, Inc., and Patrick Stack of TrueGage for technical assistance.

### **References**

1. Kinney BM. Discussion- Cellulite Treatment: A Myth or Reality: A Prospective Randomized, Controlled Trial of Two Therapies, Endermologie and Aminophylline Cream. *Plast Reconstr Surg* 1999;104(4):1115-1117.
2. Draelos ZD, Marenus KD. Cellulite. Etiology and purported treatment. *Dermatol Surg* 1997;23(12):1177-81.

3. Smith WP. Cellulite Treatments: Snake Oils of Skin Science. *Cosmetics and Toiletries* 1995;110(7):61-70.
4. Collis N, Elliot LA, Sharpe C, Sharpe DT. Cellulite treatment: a myth or reality: a prospective randomized, controlled trial of two therapies, endermologie and aminophylline cream. *Plast Reconstr Surg* 1999;104(4):1110-4; discussion 1115-7.
5. DiSalvo RM. Controlling the Appearance of Cellulite. *Cosmetics and Toiletries* 1995;110(7):50-59.
6. Bertin C, Zunino H, Pittet JC, Beau P, Pineau P, Massonneau M, et al. A double-blind evaluation of the activity of an anti-cellulite product containing retinol, caffeine, and ruscogenine by a combination of several non-invasive methods. *J Cosmet Sci* 2001;52(4):199-210.
7. Rossi AB, Vergnanini AL. Cellulite: a review. *J Eur Acad Dermatol Venereol* 2000;14(4):251-62.
8. Lucassen GW, van der Sluys WLN, van Herk JJ, Nuijs AM, Wierenga PE, Barel AO, et al. The effectiveness of massage treatment on cellulite as monitored by ultrasound imaging. *Skin Res Technol* 1997;3:154-160.
9. Perin F, Perrier C, Pittet JC, Beau P, Schnebert S, Perrier P. Assessment of skin improvement treatment efficacy using the photograding of mechanically-accentuated macrorelief of thigh skin. *International Journal of Cosmetic Science* 2000;22:147-156.
10. Hu W, Siegfried EC, Siegel DM. Product-related emphasis of skin disease information online. *Arch Dermatol* 2002;138(6):775-80.
11. Artz JS, Dinner MI. Treatment of cellulite deformities of the thighs with topical aminophylline gel. *The Canadian Journal of Plastic Surgery* 1995;3(4):190-192.
12. Hexsel DM, Mazzuco R. Subcision: a treatment for cellulite. *Int J Dermatol* 2000;39(7):539-44.
13. Kligman A, Pagnoni A, Stoudemayer T. Topical Retinol Improves Cellulite. *Journal of Dermatological Treatment* 1999;10:119-125.
14. Pierard-Franchimont C, Pierard GE, Henry F, Vroome V, Cauwenbergh G. A randomized, placebo-controlled trial of topical retinol in the treatment of cellulite. *Am J Clin Dermatol* 2000;1(6):369-74.
15. Rao J, Paabo KE, Goldman MP. A double-blinded randomized trial testing the tolerability and efficacy of a novel topical agent with and without occlusion for the treatment of cellulite: a study and review of the literature. *J Drugs Dermatol* 2004;3(4):417-25.
16. Lis-Balchin M. Parallel Placebo-controlled Clinical Study of a Mixture of Herbs Sold as a Remedy for Cellulite. *Phytotherapy Research* 1999;13:627-629.
17. Rosenbaum M, Prieto V, Hellmer J, Boschmann M, Krueger J, Leibel RL, et al. An exploratory investigation of the morphology and biochemistry of cellulite. *Plast Reconstr Surg* 1998;101(7):1934-9.
18. Rose EH, Vistnes LM, Ksander G. A Microarchitectural Model of Regional Variations in hypodermal Mobility in Porcine and Human Skin. *Annals of Plastic Surgery* 1978;2(3):252-266.
19. Nurnberger F, Muller G. So-called cellulite: an invented disease. *J Dermatol Surg Oncol* 1978;4(3):221-9.
20. Pierard GE, Nizet JL, Pierard-Franchimont C. Cellulite: from standing fat herniation to hypodermal stretch marks. *Am J Dermatopathol* 2000;22(1):34-7.
21. Dickinson BI, Gora-Harper ML. Aminophylline for cellulite removal. *Ann Pharmacother* 1996;30(3):292-3.
22. <http://www.predev.com>. Surface Metrology Guide. In; 2003.
23. Walton C, Lees B, Crook D, Worthington M, Godsland IF, Stevenson JC. Body Fat Distribution, Rather than Overall Adiposity, Influences Serum Lipids and Lipoproteins in Healthy Men Independently of Age. *The American Journal of Medicine* 1995;99:459-464.
24. Serup J, Keiding J, Fullerton A, Gniadecka M, Gniadecki R. High-frequency ultrasound examination of skin: introduction and guide. In: Serup J, Jemec BE, editors. *Handbook of Non-Invasive Methods and the Skin*. Boca Raton: CRC Press; 1995. p. 239-256.
25. Dobke MK, DiBernardo B, Thompson C, Hakan U. Assessment of biomechanical skin properties: Is cellulitic skin different? *Aesthetic Surgery Journal* 2002;22:260-267.
26. Denecker K, De Neve P, Van Assche S, Van de Walle R, Lemahieu I, Philips W. Psychovisual Evaluation of Lossy CMYK Image Compression for Printing Applications. *Computer Graphics Forum* 2002;21(1):5-17.

27. Leveque JL. EEMCO guidance for the assessment of skin topography. The European Expert Group on Efficacy Measurement of Cosmetics and other Topical Products. *J Eur Acad Dermatol Venereol* 1999;12(2):103-14.
28. Akazaki S, Nakagawa H, Kazama H, Osanai O, Kawai M, Takema Y, et al. Age-related changes in skin wrinkles assessed by a novel three-dimensional morphometric analysis. *Br J Dermatol* 2002;147(4):689-95.
29. Lagarde JM, Rouvrais C, Black D, Diridollou S, Gall Y. Skin topography measurement by interference fringe projection: a technical validation. *Skin Res Technol* 2001;7(2):112-21.
30. Fischer TW, Wigger-Alberti W, Elsner P. Direct and non-direct measurement techniques for analysis of skin surface topography. *Skin Pharmacol Appl Skin Physiol* 1999;12(1-2):1-11.
31. Jacobi U, Chen M, Frankowski G, Sinkgraven R, Hund M, Rzany B, et al. In vivo determination of skin surface topography using an optical 3D device. *Skin Res Technol* 2004;10(4):207-14.
32. Friedman PM, Skover GR, Payonk G, Kauvar AN, Geronemus RG. 3D in-vivo optical skin imaging for topographical quantitative assessment of non-ablative laser technology. *Dermatol Surg* 2002;28(3):199-204.
33. Moss JP, Ismail SF, Hennessy RJ. Three-dimensional assessment of treatment outcomes on the face. *Orthod Craniofac Res* 2003;6 Suppl 1:126-31; discussion 179-82.
34. Hennessy RJ, Lane A, Kinsella A, Larkin C, O'Callaghan E, Waddington JL. 3D morphometrics of craniofacial dysmorphology reveals sex-specific asymmetries in schizophrenia. *Schizophr Res* 2004;67(2-3):261-8.
35. Rohmer, S M-M, D M, JM S, Gharbi, P H. Fringes projection and cellulite. *Skin Research and Technology* 2004;10(4):1-16.
36. Whitestone, G G, BK M. Three-dimensional Anthropometric Techniques Applied to the Fabrication of Burn Masks and the Quantification of Wound Healing. In: SPIE; 1996; San Diego, CA; 1996.
37. Traikovich SS. Use of topical ascorbic acid and its effects on photodamaged skin topography. *Arch Otolaryngol Head Neck Surg* 1999;125(10):1091-8.
38. Mole B, Blanchemaison P, Elia D, Lafontan M, Mauriac J, Mauriac M, et al. [High frequency ultrasonography and celluscore: an improvement in the objective evaluation of cellulite phenomenon]. *Ann Chir Plast Esthet* 2004;49(4):387-95.

## Figures

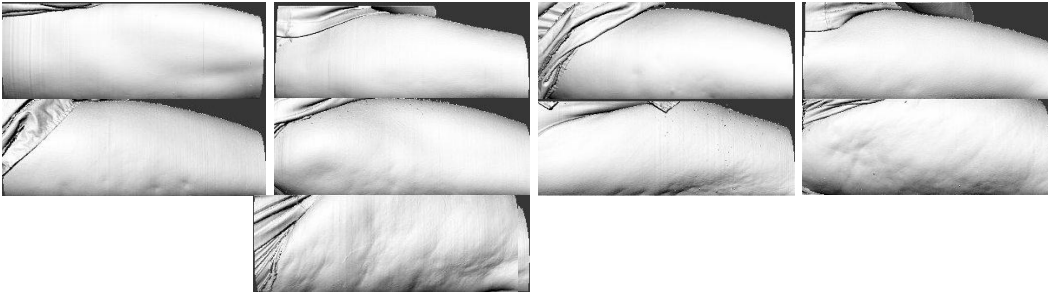


Figure 1. **Expert Image Grading Scale.** For quantitation of cellulite severity, TrueMap software analyzes the selected region of interest (ROI), creates a topographic map, and computes the standard roughness values for the surface.

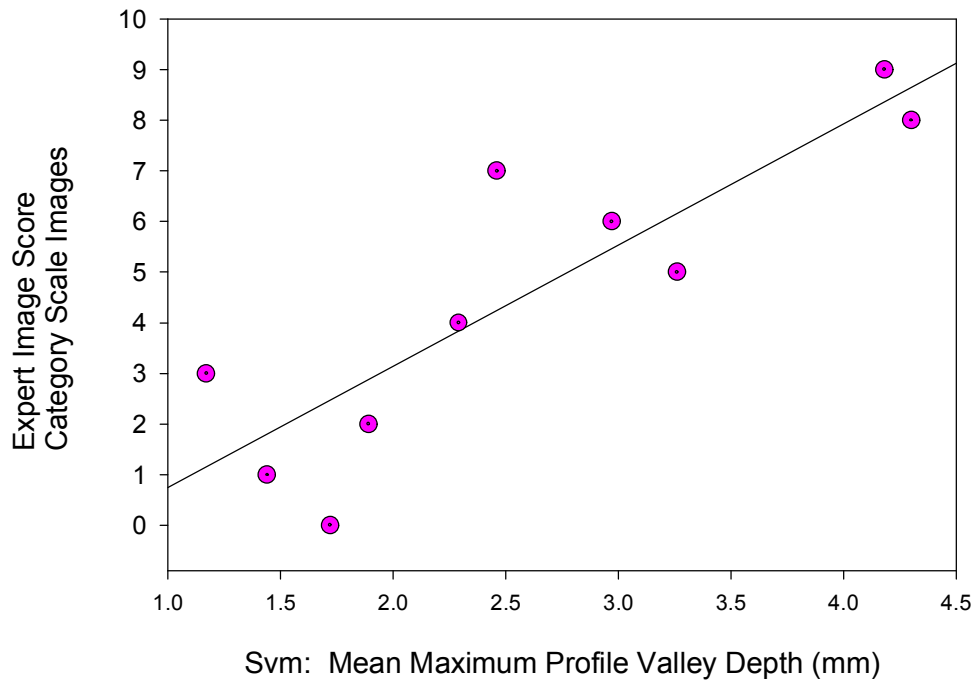
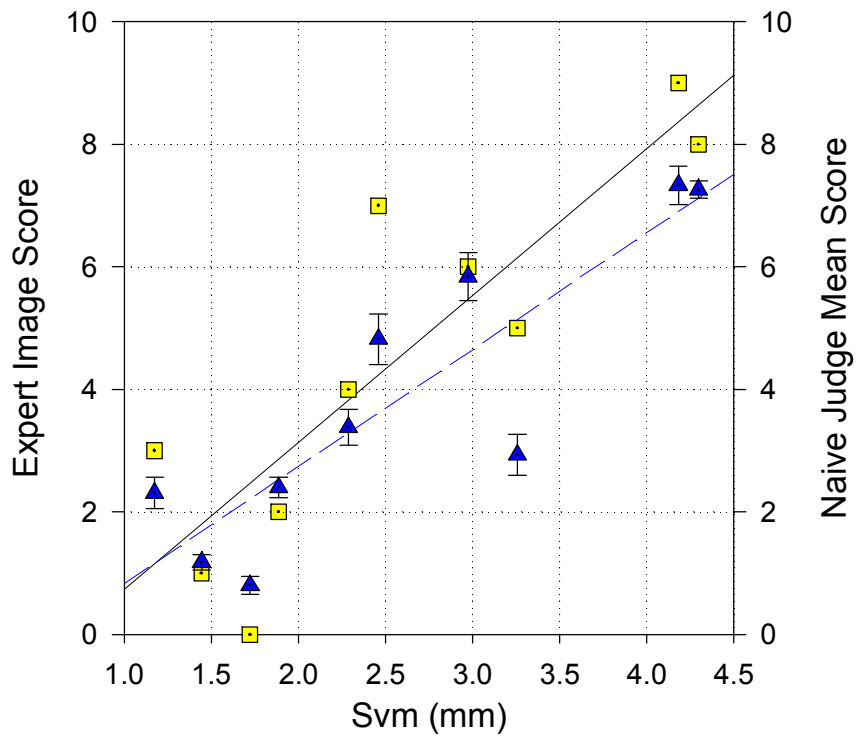
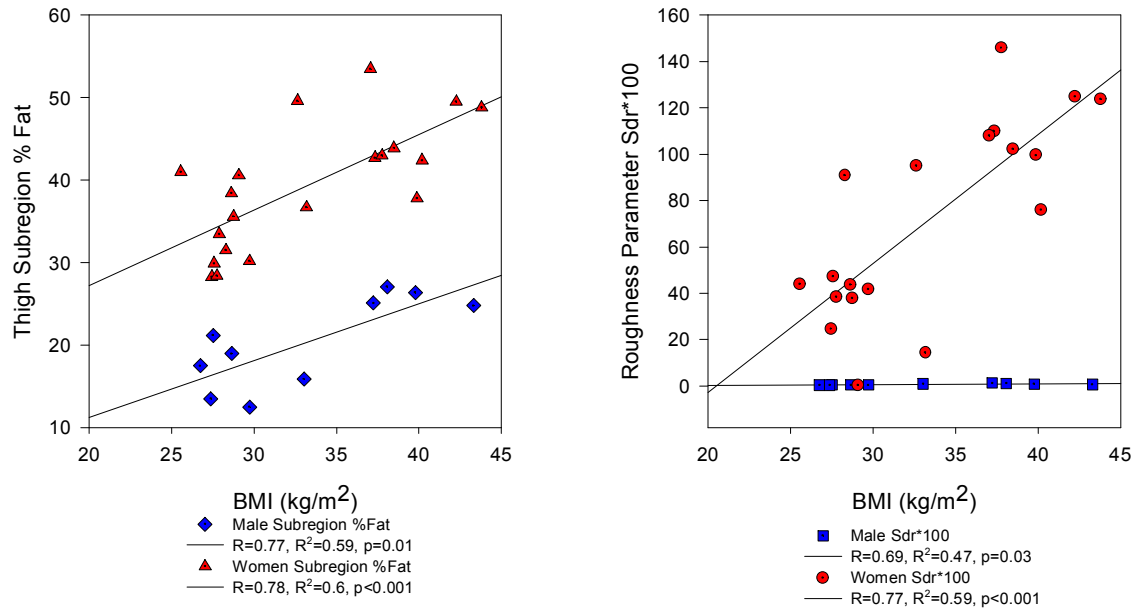


Figure 2. **Surface Roughness versus Expert Image Score.** Cellulite severity quantification by roughness parameter Svm correlates ( $r=0.86$ ,  $p=0.001$ ) to Expert Image Grade ( $n=10$ ).



**Figure 3. Quantitative Roughness Evaluation and Human Image Assessment.** Cellulite severity (Svm) vs. Expert and Naïve Judge (Mean  $\pm$  SE) Scores.



**Figure 4. Male and Female Comparisons.** Males had a significantly lower amounts of fat in the subregion of interest and significantly lower values for Sdr at comparable body mass indices. The graph shows Sdr\*100 for clarity of illustration.

Tables

**Table 1.** 3D Surface Profile Parameters (22)

Parameter	Description
<b>Sa</b>	<b>Average Roughness (mm):</b> Average of the absolute distances of the surface profile from the reference plane.
<b>Sq</b>	<b>Root-Mean-Square Roughness (mm):</b> Width or variance of the amplitude distribution function.
<b>Sp</b>	<b>Maximum Profile Peak Height (mm):</b> Height of the highest profile peak above the reference plane.
<b>Sv</b>	<b>Maximum profile Valley Depth (mm):</b> Depth of the lowest profile valley below the reference plane.
<b>St</b>	<b>Maximum Height of Profile (mm):</b> The vertical distance from the highest peak to the deepest valley ( $St = Sp + Sv$ ).
<b>Ssk</b>	<b>Skewness (mm):</b> Symmetry of the roughness profile variation about its mean.
<b>Sku</b>	<b>Kurtosis (mm):</b> Spikiness of the roughness profile.
<b>Spm</b>	<b>Mean Maximum Profile Peak Height (mm):</b> Mean height of the highest peaks over the entire surface.
<b>Svm</b>	<b>Mean Maximum Profile Valley Depth (mm):</b> Mean depth of the lowest valleys over the entire surface.
<b>Sz</b>	<b>Mean Maximum Height of Profile (mm):</b> Mean vertical distance from the highest peaks to the lowest valleys over the entire surface ( $Sz = Spm - Svm$ ).
<b>Sdr</b>	<b>Surface Area Ratio (%):</b> The ratio between the roughness surface area and the area of the flat xy plane. For a flat surface, the surface area and the xy plane area are equal, and $Sdr = 0\%$ .

**Table 2.** Ten-Point Category Scale

None	Slight Cellulite			Moderate Cellulite			Severe Cellulite		
[0]	[1]	[2]	[3]	[4]	[5]	[6]	[7]	[8]	[9]

**Table 3.** Cellulite Score Correlations to Surface Roughness Parameters (n=10)

	Visual Score	S <sub>a</sub>	S <sub>q</sub>	S <sub>p</sub>	S <sub>v</sub>	S <sub>t</sub>	S <sub>sk</sub>
<b>Expert Image Score (r, p value)</b>	0.92 0.00	0.76 0.011	0.75 0.013	0.67 0.033	0.67 0.033	0.76 0.011	0.39 0.269
<b>Live Visual Score (r, p value)</b>		0.82 0.002	0.77 0.007	0.79 0.004	0.51 0.126	0.71 0.019	0.56 0.081

	Visual Score	S <sub>ku</sub>	S <sub>pm</sub>	S <sub>vm</sub>	S <sub>z</sub>	S <sub>dr</sub>
<b>Expert Image Score (r, p value)</b>	0.92 0.00	-0.32 0.361	0.78 0.008	0.86 0.001	0.83 0.003	0.86 0.002
<b>Live Visual Score (r, p value)</b>		-0.71 0.019	0.86 0.000	0.83 0.000	0.86 0.000	0.89 0.000

**Table 4:** Morphological, Biophysical and Anthropomorphic Properties

	<b>Females</b>	<b>N = 54</b>	<b>Males</b>	<b>N = 10</b>
	Mean $\pm$ SE	Range	Mean $\pm$ SE	Range
<b>Anthropomorphic Data</b>				
Weight (lbs)	205.4 $\pm$ 7.0	128 - 331	225.6 $\pm$ 12.3	168 - 290
BMI	34.9 $\pm$ 1.2	21.3 - 56.8	33.2 $\pm$ 1.9	26.8 - 43.3
Age (years)	44.4 $\pm$ 1.2	21 - 60	41.8 $\pm$ 3.5	25 - 57
Thigh Circumference (in)	26.9 $\pm$ 0.5	21 - 35	26.0 $\pm$ 0.8	23.0 - 30.5
<b>Cellulite Morphology</b>				
Visual Grade	1.0 $\pm$ 0.2	0.0 - 4.0	0.2 $\pm$ 0.1	0.0 - 1.0
Expert Image Score	4.7 $\pm$ 0.4	0.0 - 9.0	3.8 $\pm$ 0.8	0.0 - 7.0
Sa	1.1 $\pm$ 0.1	0.3 - 2.1	0.8 $\pm$ 0.1	0.4 - 1.3
Sq	1.4 $\pm$ 0.1	0.4 - 2.6	1.0 $\pm$ 0.1	0.5 - 1.6
Sp	3.9 $\pm$ 0.2	1.2 - 8.7	3.4 $\pm$ 0.4	1.8 - 5.9
Sv	5.2 $\pm$ 0.3	1.5 - 12.9	4.4 $\pm$ 0.5	2.7 - 8.0
St	9.1 $\pm$ 0.4	3.1 - 17.9	7.8 $\pm$ 0.8	5.0 - 12.8
Ssk	-0.2 $\pm$ 0.1	-1.5 - 0.8	-0.2 $\pm$ 0.1	-1.2 - 0.1
Sku	3.8 $\pm$ 0.2	2.2 - 7.1	4.2 $\pm$ 0.7	2.3 - 8.9
Spm	2.6 $\pm$ 0.1	1.0 - 4.8	2.1 $\pm$ 0.2	1.2 - 3.4
Svm	2.8 $\pm$ 0.2	1.0 - 7.1	2.3 $\pm$ 0.2	1.7 - 3.6
Sz	5.4 $\pm$ 0.3	2.0 - 11.8	4.4 $\pm$ 0.4	2.9 - 6.6
Sdr	0.9 $\pm$ 0.1	0.0 - 3.3	0.01 $\pm$ 0.00	0.00 - 0.01
<b>Body Composition</b>				
% Fat Thigh	44.4 $\pm$ 1.0	28.8 - 56.6	20.3 $\pm$ 1.7	12.5 - 27.1
% Lean Thigh	53.6 $\pm$ 0.9	42.0 - 69.1	29.0 $\pm$ 1.9	19.9 - 37.0
% Fat Subregion	36.8 $\pm$ 1.2	18.5 - 53.7	68.5 $\pm$ 1.8	61.2 - 77.1
<b>3D Ultrasound</b>				
Dermal Thickness	1.5 $\pm$ 0.0	1.2 - 2.1	1.7 $\pm$ 0.1	1.2 - 2.0
Ultrasound Surface Area	352 $\pm$ 8	259 - 470	355 $\pm$ 20	283 - 460
Surface Texture With Photography				
Red Band SD	14.8 $\pm$ 0.5	6.8 - 22.7	14.9 $\pm$ 1.6	9.7 - 24.0
<b>Biomechanical Properties</b>				
Laxity	1.1 $\pm$ 0.0	0.6 - 1.8	1.0 $\pm$ 0.1	0.7 - 1.3
Laxity %	62.0 $\pm$ 0.9	41.8 - 72.3	60.9 $\pm$ 2.2	50.3 - 69.6
Elastic Deformation	1.8 $\pm$ 0.0	1.2 - 2.6	1.7 $\pm$ 0.1	1.4 - 2.0
Stiffness	143 $\pm$ 2	115 - 176	146 $\pm$ 4	125 - 158
Energy Absorption	91.2 $\pm$ 1.4	67.3 - 121.4	87.9 $\pm$ 2.9	78.2 - 99.4
Elasticity mm	1.0 $\pm$ 0.0	0.6 - 1.5	1.0 $\pm$ 0.1	0.8 - 1.4
% Elasticity	55.3 $\pm$ 0.8	43.1 - 70.8	58.4 $\pm$ 2.0	51.7 - 68.2

**Table 5:** Significant Correlations  $\approx 0.4$  or Higher (n = 56 subjects)

<b>Parameter</b>	<b>Positively Correlated With....</b>
Expert Image Score	BMI, weight, thigh circumference, Svm, Sz, Spm, Sa, Sq, Sp, St, visual grade, thigh % fat, thigh subregion % fat, red band SD, energy absorption
Svm	BMI, weight, thigh circumference, expert image score, visual grade, thigh % fat, thigh subregion % fat, ultrasound surface area, stiffness (neg), energy absorption, red band SD
Sz	BMI, weight, thigh circumference, expert image score, visual grade, thigh % fat, thigh subregion % fat
Visual Grade	BMI, weight, thigh circumference, Sa, Sq, Spm, Svm, Sz, thigh % fat, thigh subregion % fat, ultrasound surface area, red band SD, stiffness (neg), energy absorption
Age	% elasticity (neg)
Thigh Subregion % Fat	BMI, weight, thigh circumference, Sa, Sq, St, Spm, Svm, thigh % fat, ultrasound surface area, red band SD, elastic deformation, energy absorption
Ultrasound Surface Area	BMI, weight, thigh circumference, Svm, Sz, thigh % fat, red band SD, elastic deformation, energy absorption, stiffness (neg)
Elastic Deformation	BMI, weight, thigh circumference, Spm, thigh % fat, ultrasound surface area, laxity %, laxity (mm), stiffness (neg), energy absorption, elasticity (mm)
Energy Absorption	BMI, weight, thigh circumference, St, Spm, Svm, Sz, thigh % fat, ultrasound surface area, laxity (mm), elastic deformation, stiffness (neg), elasticity (mm)

\*Negative Correlation- (neg)